UBVRI PHOTOMETRY OF THE TYPE Ia SN 1994D IN NGC 4526

MICHAEL W. RICHMOND
Department of Astrophysical Sciences, Princeton University, Princeton, New Jersey 08544

RICHARD R. TREFFERS, ALEXEI V. FILIPPENKO,[1] SCHUYLER D. VAN DYK, YOUNG PAIK, AND CHIEN PENG
Department of Astronomy, University of California at Berkeley, Berkeley, California 94720

LAURENCE A. MARSCHALL AND BENTLEY D. LAAKSONEN
Department of Physics, Gettysburg College, Gettysburg, Pennsylvania 17325

BRUCE MACINTOSH AND IAN S. MCLEAN
Department of Astronomy, University of California at Los Angeles, Los Angeles, California 90024

Received 1994 September 26, revised 1995 January 18

ABSTRACT

We present optical photometry for the type Ia SN 1994D in NGC 4526 from 1994 March 7 to June 4 starting 13 days before *B*-band maximum. The light curves of this SN resemble closely those of the "normal" type Ia events SNe 1989B and 1980N, differing only in a slightly faster decline after maximum in *VRI*. The optical absolute magnitudes of SN 1994D, however, are significantly brighter than those of its near twins, and brighter than those predicted by Phillips' [ApJ, 413, L105 (1993)] relationship between decline rate and luminosity. Our small amount of IR photometry of SN 1994D is not inconsistent with that of other type Ia SNe.

1. INTRODUCTION

SN 1994D in the S0 galaxy NGC 4526 was discovered by the Leuschner Observatory Supernova Search (LOSS) in an image taken on 1994 March 7 UT (Treffers *et al.* 1994), the sixth SN to be discovered by LOSS since its inception in late 1992. Optical spectra obtained shortly after discovery identify the event as a type Ia, defined by a lack of hydrogen and the presence of a strong absorption trough due to Si II near 6150 Å. Argyle & Morrison (1994) have measured an accurate position of $\alpha = 12^h34^m02^s.395$, $\delta = +07°42'05''.07$ (equinox J2000.0, FK5 reference frame), 9".0 west and 7".8 north of the nucleus. We immediately began a program of multicolor photometry, and report here on the results from the first 89 days of observation at three sites.

Section 2 contains a description of the observations and analysis; we compare several methods for performing photometry in the complicated area surrounding SN 1994D. Our calibration of the measurements onto the standard Johnson–Cousins system appears in Sec. 3. Since type Ia SNe have been proposed as "standard candles" which may be used to determine distances, we compare SN 1994D closely with two "normal" examples, SNe 1989B and 1980N. In Sec. 4 we present their light curves, and in Sec. 5 their color curves. Near-IR photometry of SN 1994D appears in Sec. 6. After estimating the extinction to SN 1994D in Sec. 7, we calculate absolute magnitudes in all passbands in Sec. 8. In Sec. 9, we use these values to test the hypothesis of Phillips (1993; hereafter referred to as P93) that type Ia SN absolute magnitudes are correlated with their rate of decline. An Appendix describes briefly the color terms used to place the Leuschner Observatory data onto the standard system.

2. OBSERVATIONS AND REDUCTION

Figure 1 shows SN 1994D, its host galaxy NGC 4526, and reference stars A, B, and C. We include observations from four instruments: two telescopes at Leuschner Observatory in northern California, one at the National Undergraduate Research Observatory (NURO) near Flagstaff, AZ, and the Lick Observatory 3 m Shane telescope.

At Leuschner Observatory, we used a 50 and a 76 cm telescope, both reflectors equipped with CCD cameras (Richmond *et al.* 1993; Richmond *et al.* 1994, hereafter referred to as R94). The full width at half-maximum (FWHM) of stellar images was usually 3"–4", but worse on a small number of nights. We created bias frames by taking the median of five images each afternoon, and flatfield frames from the median of five exposures of the twilight sky; we then applied them to the raw images in the usual fashion.

Measuring the light of the SN was not straightforward: due to the large seeing disk and the proximity of the SN to the bright nucleus and dust lane of NGC 4526, we found that simple aperture photometry usually produced unreliable results. In the *U*-band, however, where the images had a low signal-to-noise ratio [no star in our field was bright enough to serve as a model for the point-spread function (PSF)], and we barely detected light from the nucleus, we judged it the best method. Therefore, our *U*-band magnitudes are based on photometry using circular apertures of radius 3".1.

[1]Also associated with the Center for Particle Astrophysics, University of California at Berkeley.

 0004-6256/95/109(5)/2121/13/$0.90

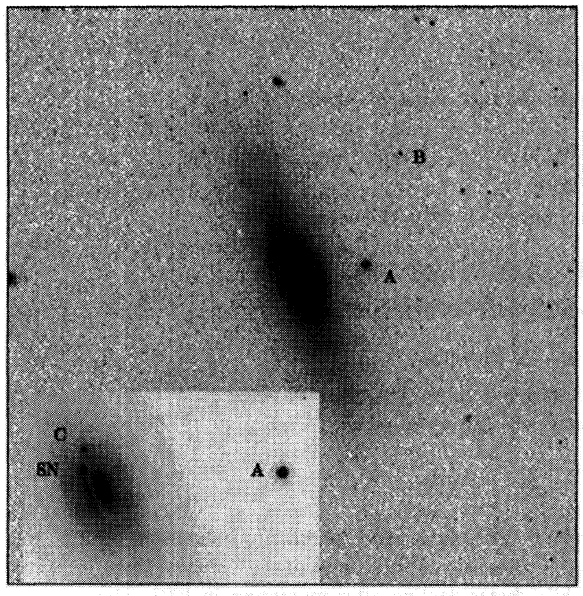

FIG. 1. Field of NGC 4526, with inset showing central regions. West is up and north to the left. The field of view is about 10′×10′.

For all the other passbands, in order to remove the gradient around the SN due to the smoothly distributed light of the galaxy, we tested two methods of extracting instrumental magnitudes, in addition to simple aperture photometry. The first one, which we call "rotation," could be used immediately after we acquired images of the object. We rotated a copy of each image by 180° around the center of the nucleus, and then subtracted the copy from the original [as described in Filippenko *et al.* (1992)]. However, the prominent dust lane near the nucleus introduced an asymmetry that led to significant positive and negative residuals in the subtracted image (see Fig. 2). Using pre-explosion images taken with the 76 cm telescope in the *R*-band, we determined that the remaining background light at the position of the SN was about one-third that of the maximum positive residual (due

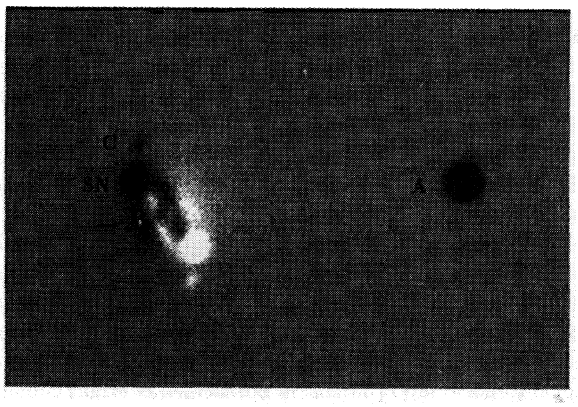

FIG. 2. Central region of NGC 4526 after a rotated copy of the image has been subtracted from the original. The dark area indicated by the arrow was used to find a "sky" value for the SN (see the text). West is up and north to the left. The field is 157″×106″ in size.

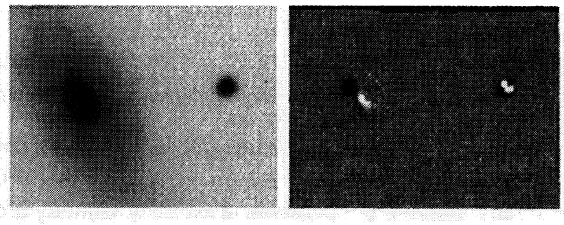

FIG. 3. The left-hand panel shows an *R*-band image of the central portion of NGC 4526 taken on 1994 May 2 UT. The right-hand panel shows the same image after a scaled template image taken 1994 November 13 UT has been subtracted; black regions represent positive residuals and white regions negative residuals. The displayed values are the square root of true intensity in both panels. West is up and north to the left. Each panel is approximately 160″×130″ in size.

north of the nucleus), where both were measured as the median of values in a 3.″4×3.″4 box. Assuming that this ratio of residual backgrounds is *the same in all passbands as in R*, we determined an effective "sky" value at the position of the SN in all images as one-third of the peak positive residual in the subtracted image. Finally, we applied the IRAF[2] implementation of DAOPHOT (Stetson 1987) to the subtracted image, using star A to determine the PSF and setting the sky value for the SN to that determined above. The DAOPHOT task NSTAR produced a set of differential raw magnitudes for the SN and reference stars A, B, and C (in some images, B and C were too faint to be detected).

In 1994 November and December, after the SN had faded into invisibility from our site, we acquired additional images of NGC 4526 with both telescopes in order to perform another method of extracting magnitudes. In the "template" method (e.g., Filippenko *et al.* 1986), we matched a late-time image (the template) of the galaxy to each early image, shifting the template to align stars A and B and the galaxy's nucleus. Next, we convolved whichever image had better seeing with a Gaussian in order to match the widths of the PSF in each. We measured the brightness of star A in an aperture about 3″ in radius in each image and scaled the template to match the early image. At this point, we measured the brightness of star A in the early image using aperture photometry with a radius of 0.75×FWHM. We subtracted the template image from the earlier image, leaving only the SN and small residuals at the positions of each star (see Fig. 3). We then measured the light from the SN (in the subtracted image) via aperture photometry, again using a circular aperture of radius 0.75×FWHM. The difference between the measurements of star A and the SN we denote as our template differential magnitudes.

Comparing the different methods, we find that, while there is a large difference between the results of simple aperture photometry on the original images and those of the more complicated methods, rotation and template yield similar values. In Fig. 4, we plot the differences between the three methods for data in one passband from one telescope

[2]IRAF is distributed by the National Optical Astronomy Observatories, which are operated by the Association of Universities for Research in Astronomy, Inc., under contract to the National Science Foundation.

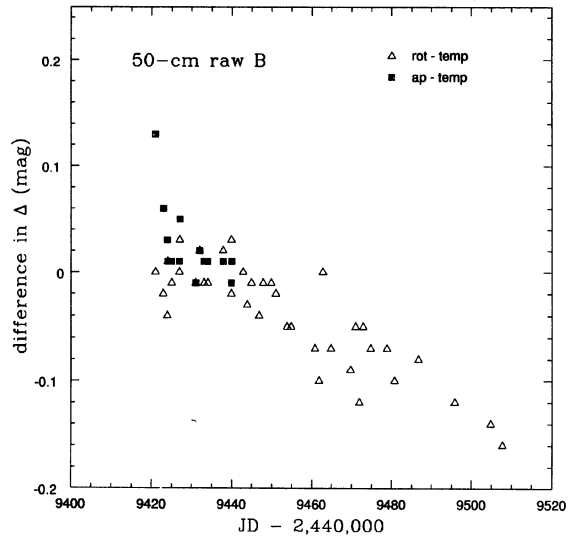

FIG. 4. An example of the difference between three methods of extracting instrumental magnitudes from images. We calculate the quantity Δ=mag(starA)−mag(SN 1994D) via methods "ap" (simple aperture photometry), "rot" (180-degree rotation, subtraction, and PSF fitting), and "temp" (template-subtraction), then plot the difference between the results as a function of time.

(which resemble results in other passbands, and from both telescopes). It is clear that pure aperture photometry yields SN magnitudes which are significantly fainter at very early times, when the SN is faint, undoubtedly due to improper subtraction of the background value. On the other hand, the other two methods agree to within less than 0.05 mag until well past maximum light (13 days for I-band with the 50 cm telescope, at least 25 days for other passbands with both telescopes), when systematic differences begin to appear. The trend is usually for the rotation method to yield a brighter SN at late times. Which of the two is better? We believe that the template method yields more reliable results for two reasons. First, we performed tests with artificial stars added to some of our very late images at the position of SN 1994D, and found that the template method was significantly more accurate when the artificial star was 2–3 mag fainter than star A. Second, the light curves made with the rotation method show more scatter around a smooth decline at late times than those made with the template method. We therefore adopt the template magnitudes as the Leuschner Observatory values throughout this paper. However, we point out that the rotation method can yield accurate results when an object is relatively bright (even if it is immersed in very complicated surroundings) and does allow quick analysis of a newly discovered supernova for which one has no template image.

We next transformed the raw magnitudes onto the Johnson–Cousins system, using observations of the M67 "dipper" asterism and the photometry listed in Richmond (1994). In a previous paper on SN 1993J (R94), we based color transformations on the R-band, which usually yields the highest signal with the Leuschner instruments. However, as the referee of the present paper pointed out, the R passband is difficult to reproduce with optical glass and CCDs, largely due to its extended tail at the red end; the standard V and I passbands are easier to match. The R-band light curve of SN 1993J clearly shows the effect of passband mismatches, with parallel tracks of data from two different instruments. Therefore, we derived new color transformation coefficients for the Leuschner telescopes, using V as the primary passband; see the Appendix. The size of the corrections was typically less than 0.1 mag.

We denote by the term "NURO" observations made with the Lowell Observatory 79 cm telescope and a Photometrics CCD camera owned by the National Undergraduate Research Observatory [see Romanishin *et al.* (1994) for details on the equipment]. The plate scale was $0\farcs49$ pixel^{-1}, and the seeing typically had a FWHM of $2\farcs5$–$3\farcs5$. After the normal bias subtraction and flatfielding, a copy of each image was rotated around the nucleus of NGC 4526, as described above, and subtracted from the original. Raw differential magnitudes for the SN and star A were determined by aperture photometry, using the IRAF task APPHOT; the aperture radius was 1.0×FWHM and the sky annulus 2.5×FWHM to 3.5 ×FWHM. The raw magnitudes were corrected for extinction and transformed to the Johnson–Cousins system using relationships derived from observations of the M67 dipper asterism, again using the photometry described in Richmond (1994). We applied the second-order color-dependent extinction term to the NURO B-band data, as described in the Appendix.

We have a small number of observations made at near-infrared wavelengths with the 3 m Shane reflector at Lick Observatory and the UCLA two-channel "Gemini" camera (McLean *et al.* 1994), an imaging system with 256×256 elements. We observed in the J, H, and K bands as follows: we took short (6–15 s) exposures of the SN, coadding 4–10 such frames into a single "object" image. Repeating this procedure three times, with $10''$ E/W offsets between each image, we compiled three images of the SN in each band. In addition, we observed three slightly offset positions about $4'$ south of the galaxy for equivalent lengths of time to create three sky images at each wavelength. The three sky images were then combined to create a median sky image in each band. This median image was subtracted from the on-source images. Finally, the resulting sky-subtracted images were divided by a flatfield frame constructed from observations of the sky taken later in the night, yielding three corrected images of SN 1994D in each bandpass for each night. We analyzed the images in the same manner as the NURO data, by rotating a copy of each image around the center of NGC 4526 and subtracting this rotated copy from the original. We measured the light of the SN in the subtracted image via aperture photometry using the APPHOT package within IRAF. The images typically had FWHM $1\farcs5$. To measure the SN and star A, we used an aperture with radius $1\farcs4$ and an annulus with radii $1\farcs4$–$2\farcs1$ to measure the sky background.

It is possible that the H-band observations of comparison star A made on March 27 may be slightly saturated. Note also that the March 27 dataset includes measurements in K-band (2.2 μm), whereas the June 18 dataset has measurements in K' (2.1 μm). We will treat the two as equivalent.

TABLE 1. Johnson–Cousins magnitudes of comparison stars.

star	U	B	V	R	I	source
A	—	13.74	12.62	—	—	Hanes et al. 1976
A*	14.54	13.57	12.54	11.98	11.51	Kilkenny & Malcolm 1984
A	—	13.61	12.56	12.04	11.61	Prugniel & Heraudeau 1994
B	—	17.06	16.09	15.43	14.88	Leuschner 50-cm
B	—	—	—	15.47	14.88	Leuschner 76-cm
C	—	16.79	16.20	15.85	15.53	Leuschner 50-cm
C	—	—	—	15.89	15.48	Leuschner 50-cm

*Adopted as primary comparison star values.

3. CALIBRATION

We have adopted star A (see Fig. 1) as our primary comparison star; the fainter stars B and C provide checks on the lack of variation of star A, and yield estimates of the precision of photometry of the SN. The magnitude of star A has been measured by several observers. We list in Table 1 three sets of measurements, which show agreement to better than 0.1 mag [with the single exception of the B-band measurement of Hanes *et al.* (1976)]. We have adopted the values of Kilkenny & Malcolm (1984) for use throughout this paper. Although they made only a single measurement in each passband, the fact that their data agree well with the independent measurements of Prugniel & Heraudeau (1994) gives us confidence in the results.

In the IR, we were unable to find previous photometry of star A. The March 27 UT observations of the UKIRT faint standards FS21 and FS12 (Casali & Hawarden 1992) were used to determine the magnitudes of star A in JHK, which we list in Table 2; we used these magnitudes in reducing the June 18 data. The estimated uncertainties in Table 2 are a combination of uncertainties induced by photon noise and residual flatfielding errors (which dominate in K), and uncertainties in the tabulated magnitudes of the UKIRT standards (which dominate in J); our H-band measurements may suffer from slight saturation and detector nonlinearity, which are difficult to detect in our mode of observation.

We can determine the internal precision of our measurements, and verify that our primary standard did not vary over the period of observations, by measuring the difference between star A and the fainter stars B and C. Note that star C is immersed in the light of NGC 4526, not far from the position of SN 1994D, and is roughly as bright as the isolated star B. We claim that the difference in the precision to which we can measure these two comparison stars indicates roughly the degree to which the galaxy's light affects our measurements of SN 1994D. Using the Leuschner 50 cm ($BVRI$) and 76 cm (RI only) observations, we have measured the differences between the raw instrumental magnitudes of stars A, B, and C. We list in Table 3 the standard deviation from the mean of these differences (the color-corrected mean differences can be derived from Table 1). It is clear that the galaxy's light makes photometry significantly less precise: in VRI, the standard deviations in measurements of star C are four to seven times larger than those of star B. We believe that the figures for star C provide an indication of the uncertainty in our measurements of SN 1994D at *late* times; at early times, the SN was so much brighter that the uncertainty is only a few hundredths of a magnitude. There was no indication of any long-term trend in the brightness of star A relative to star B of more than 0.02 mag over a period of 89 days, nor any indication of periodicity.

TABLE 2. IR magnitudes of comparison stars.

star	J	H	K	source
A*	10.74 ± 0.03	10.39 ± 0.05	10.13 ± 0.02	Lick IR (see text)

*Adopted as primary comparison star values.

TABLE 3. Internal accuracy of differential magnitudes.

difference	B	V	R	I	telescope
A-B	0.20	0.06	0.03	0.04	Leuschner 50-cm
A-B	—	—	0.08	0.05	Leuschner 76-cm
A-C	0.15	0.29	0.22	0.18	Leuschner 50-cm
A-C	—	—	0.44	0.30	Leuschner 76-cm

The U-band data may have significant systematic errors. Our U-band images had by far the lowest signal-to-noise ratios. Moreover, we used a calibration field (PG 1633+009; Landolt 1992) containing only a single star with a $(U-B)$ color more negative than that of the SN at maximum light to derive the color-transformation coefficients. It is possible that the different methods of photometry for U and B may have introduced a systematic error in the U-band magnitudes, although a comparison of simple aperture photometry and the rotation procedure described above yielded similar results in the B-band at the time of maximum light. We were unable to find independent U-band measurements simultaneous with ours, but several measurements in the days just before our first U-band data appear in the IAU Circulars. Table 4 shows that other observers found smaller $(U-B)$ colors than those we measured shortly thereafter. We feel it not unlikely that our U-band measurements may be systematically too bright by up to 0.5 mag. However, our measurements provide a qualitative description of the shape of the U-band light curve of a type Ia SN, and we therefore include them. We urge readers to check the literature carefully for superior U-band data from other sites.

4. OPTICAL LIGHT CURVES

In Fig. 5 we present the $UBVRI$ light curves in a single graph, and in Figs. 6, 7, 8, 9, 10 each passband separately.

TABLE 4. U and B magnitudes of SN 1994D at early times.

UT Date	U	B	U-B	source
Mar 10.2	13.22	13.62	−0.40	Walker 1994
Mar 10.16	13.4	13.7	−0.3	Shanks et al. 1994
Mar 11.17	12.8	13.3	−0.5	Shanks et al. 1994
Mar 12.4	11.92	12.89	−0.97	this paper
Mar 13.4	11.76	12.61	−0.85	this paper

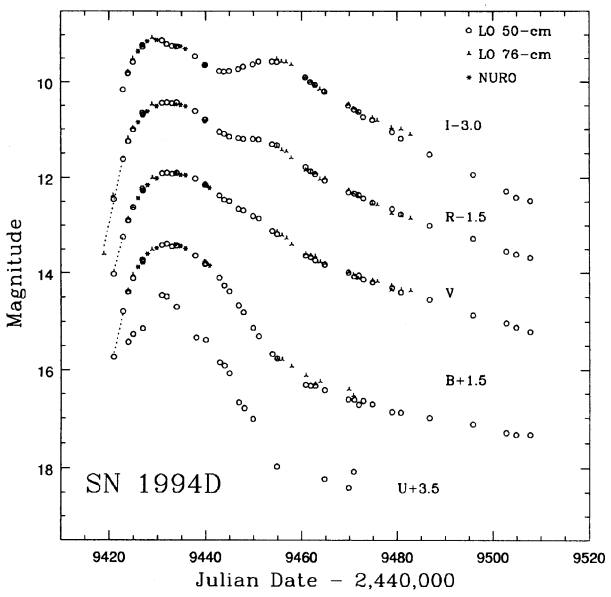

FIG. 5. *UBVRI* light curves of SN 1994D.

Tables 5, 6, and 7 contain the data from the Leuschner 50, 76 cm, and NURO telescopes, respectively. After calculating the times and magnitudes at peak, we will discuss each light curve in turn, comparing it with those of other type Ia SNe. The light curves we present, obtained entirely with small telescopes (apertures less than 1 m), provide some of the best coverage of the early photometric evolution of a type Ia SN in the literature.

The times and magnitudes of the peak in each band are listed in Table 8. In order to determine these, we attempted to fit a parabola to the light curve in each passband, using data from all telescopes within a short time around the peak. However, our efforts led us to believe that this method is inappropriate for three reasons. First, the time of peak, and its value, changed significantly when the time interval included in the fit was increased or decreased; the values did not converge in any obvious way. Second, the shapes of the R-band and I-band light curves, especially, are clearly not parabolic near peak, and showed large, systematic residuals from the best fits. Finally, the fitted times of maximum light differed by at least half a day from the times estimated by eye, a discrepancy too large for us to accept. We conclude that a parabola is simply not an appropriate model for the light curve of SN 1994D near its peak. Therefore, we estimated magnitudes at the peak of each light curve by eye; note that these are always within 0.01 mag of the brightest datum. To determine the times of maximum light, we performed a Monte Carlo experiment: we selected all data points between March 14 and March 28 UT, inclusive. We assigned a random error to each observed magnitude, drawn from a normal distribution with σ=0.05, 0.01, 0.02, 0.01, 0.01 mag, for U, B, V, R, and I, respectively. We then smoothed the data with a cosine filter of width 4.0 days, and found the time at which the smoothed magnitudes reached a minimum. After repeating this process 1,000 times for each

TABLE 5. Leuschner 50-cm data on SN 1994D.

UT Date	JD[a]	U	B	V	R	I	conditions
Mar 09.40	9420.90	—	14.23	14.02	13.95	—	thin clouds
Mar 11.53	9422.83	—	13.29	13.24	13.12	13.16	thin clouds
Mar 12.40	9423.90	11.92	12.89	12.89	12.75	12.81	
Mar 13.39	9424.89	11.76	12.61	12.62	12.50	12.58	
Mar 15.40	9426.90	11.64	12.26	12.27	12.19	12.26	clouds
Mar 19.39	9430.89	10.96	11.91	11.91	11.94	12.12	clouds
Mar 20.35	9431.85	10.99	11.88	11.90	11.93	12.20	
Mar 21.48	9432.98	—	11.94	11.92	11.95	12.24	thin clouds
Mar 22.40	9433.90	11.20	11.92	11.90	11.93	12.25	thin clouds
Mar 26.47	9437.97	11.83	12.13	12.02	12.11	12.46	clouds
Mar 28.42	9439.92	11.88	12.30	12.14	12.29	12.64	clouds
Mar 31.34	9442.84	12.34	12.60	12.37	12.55	12.77	
Apr 01.34	9443.84	12.41	12.76	12.46	12.59	12.78	thin clouds
Apr 02.33	9444.83	12.57	12.88	12.49	12.65	12.77	
Apr 04.31	9446.81	13.17	13.17	12.65	12.68	12.73	
Apr 05.45	9447.95	13.29	13.31	12.68	12.70	12.68	
Apr 07.27	9449.77	13.51	13.63	12.80	12.70	12.63	clouds
Apr 08.46	9450.96	—	13.80	12.85	12.71	12.57	
Apr 11.29	9453.79	—	14.17	13.11	12.81	12.57	
Apr 12.26	9454.76	14.47	14.26	13.18	12.83	12.58	
Apr 18.23	9460.73	—	14.81	13.63	13.28	12.90	
Apr 19.25	9461.75	—	14.83	13.66	13.37	13.00	
Apr 20.24	9462.74	—	14.83	13.73	13.43	13.06	poor seeing
Apr 22.26	9464.76	14.72	14.92	13.82	13.56	13.20	
Apr 27.35	9469.85	14.90	15.11	13.99	13.80	13.50	poor seeing
Apr 28.38	9470.88	14.57	15.12	14.07	13.83	13.58	thin clouds
Apr 29.37	9471.87	—	15.22	14.05	13.86	13.63	
Apr 30.31	9472.81	—	15.14	14.13	13.93	13.74	clouds
May 02.22	9474.72	—	15.21	14.19	14.02	13.80	
May 06.33	9478.83	—	15.37	14.30	14.15	14.05	thin clouds
May 08.18	9480.68	—	15.38	14.40	14.26	14.19	
May 14.20	9486.70	—	15.49	14.55	14.50	14.52	
May 23.27	9495.77	—	15.62	14.87	14.77	14.94	clouds
May 30.23	9502.73	—	15.79	15.03	15.04	15.28	
Jun 01.27	9504.77	—	15.83	15.12	15.10	15.41	poor seeing
Jun 04.22	9507.72	—	15.83	15.21	15.17	15.48	

[a]Julian Date - 2,440,000.

light curve, we calculated the mean and standard deviation of the resulting distribution of peak times, and list them in Table 8. Since this smoothing procedure introduces a systematic error to the peak magnitudes (always producing too faint a peak), we use it to determine the times of maximum light only. The calculated times agree with those estimated by eye to within the uncertainties.

Let us consider the light curves in each bandpass; we will plot each one in a differential form, with time since the maximum in the B-band on the abscissa and magnitude relative to the peak value on the ordinate. We use the times and peak values listed in Table 8 to convert the observed data of SN 1994D to this coordinate system. Together with data for SN 1994D, we plot light curves for other well-observed type Ia SNe: SN 1989B (Wells *et al.* 1994, hereafter referred to as W94) and SN 1980N (Hamuy *et al.* 1991), both of which are "normal" type Ia events (i.e., exhibiting neither peculiar spectra nor abnormal light curves). We use the time at B-band maximum as the fiducial time in all figures, using our own value for SN 1994D, the time calculated by W94 for SN 1989B, and the time calculated by Hamuy *et al.* for 1980N.

The U-band light curve (Fig. 6) is sparse, and the uncertainties relatively large, especially at late times. We have

TABLE 6. Leuschner 76-cm data on SN 1994D.

UT Date	JD[a]	B	V	R	I	conditions
Mar 01.27	9412.77	—	—	≥ 18.5	—	(not detected)
Mar 07.42	9418.92	—	—	15.09*	—	
Mar 09.24	9420.74	—	—	13.87*	—	thin clouds
Mar 12.39	9423.89	12.86	12.85	12.68	12.78	
Mar 13.39	9424.89	12.53	12.61	12.47	12.50	
Mar 17.40	9428.90	12.00	12.00	11.97	12.06	
Apr 12.31	9454.81	14.26	13.12	12.86	12.51	
Apr 13.31	9455.81	14.28	13.20	12.93	12.57	
Apr 14.31	9456.81	—	13.26	12.96	12.58	poor seeing
Apr 15.30	9457.80	14.42	13.39	13.09	12.63	
Apr 18.31	9460.81	14.61	13.59	13.34	12.90	
Apr 19.30	9461.80	—	13.62	13.39	12.99	
Apr 20.28	9462.78	14.79	13.64	13.41	13.06	poor seeing
Apr 21.28	9463.78	14.74	13.76	13.53	13.15	
Apr 22.29	9464.79	—	13.80	13.51	13.22	
Apr 27.27	9469.77	14.90	13.98	13.76	13.47	poor seeing
Apr 28.27	9470.77	15.03	14.03	13.82	13.55	thin clouds
Apr 29.27	9471.77	—	14.11	13.88	13.63	
May 02.26	9474.76	—	14.15	14.04	13.75	
May 03.25	9475.75	—	14.17	14.06	13.81	
May 06.24	9478.74	—	14.26	14.24	13.96	clouds
May 08.24	9480.74	—	14.34	14.19	13.89	
May 10.23	9482.73	—	14.36	14.34	14.10	

[a]Julian Date - 2,440,000.
*Used extrapolated and/or 50-cm colors for color corrections.

chosen to use the first observed point for SN 1989B as its peak, although it is possible that it was already on the decline in the U-band when discovered. The curves are not significantly different; all reach a maximum several days before the B-band, and decline sharply, over 2.0 mag in the first 15 days after the B-band peak. It is possible that SN 1994D fades a bit more quickly than SN 1989B, but it is difficult to be sure without a well-determined peak value for the latter.

The B-band light curve (Fig. 7) is again similar to that of normal type Ia SNe. The peak is only slightly asymmetric, and falls cleanly to a fairly well-defined "knee" at about 30 days after maximum. Following P93, we define the parameter $\Delta m_{15}(X)$ to be the difference between the magnitude at peak in the X passband, and 15 days after the peak in the X passband. Using our data in the B-band, we find $\Delta m_{15}(B)=1.31\pm0.08$ mag for SN 1994D, where the uncertainty is the sum in quadrature of the uncertainty in the B-band peak magnitude and the change in the interpolated magnitude 15 days after peak if the date of maximum is changed by the amount listed in Table 8. This is the same, to

TABLE 7. NURO data on SN 1994D.

UT Date	JD[a]	B	V	R	I
Mar 14.41	9425.91	12.37	12.43	12.35	12.35
Mar 15.90	9426.90	12.28	12.28	12.21	12.22
Mar 16.37	9427.87	12.09	12.15	12.12	12.14
Mar 18.27	9429.77	11.97	12.02	12.01	12.11
Mar 22.25	9433.75	11.89	11.91	11.97	12.23
Mar 23.25	9434.75	11.93	11.94	11.98	12.25
Mar 24.28	9435.78	11.98	11.95	12.01	12.30
Mar 28.32	9439.82	12.25	12.15	12.33	12.63
Mar 29.25	9440.75	12.34	12.21	—	—

[a]Julian Date - 2,440,000.

TABLE 8. Peak apparent magnitudes of SN 1994D.

	U	B	V	R	I
Date[a]	9431.6 ± 0.9	9432.0 ± 0.5	9432.4 ± 0.6	9431.8 ± 0.1	9429.1 ± 0.3
Mag[b]	10.96 ± 0.3	11.89 ± 0.02	11.90 ± 0.02	11.92 ± 0.02	12.06 ± 0.05

[a]Julian Day - 2,440,000.
[b]Peak of smooth curve through data points.

within the uncertainties, as SN 1980N's $\Delta m_{15}(B)=1.28\pm0.05$ mag or SN 1989 B's $\Delta m_{15}(B)=1.31\pm0.07$ mag, and places SN 1994D's value well within the middle of the distribution of $\Delta m_{15}(B)$ for all SNe Ia (P93). Note that the exponential-decay portion of SN 1994D's light curve is about 0.25 mag farther below the peak than that of the other two SNe.

In the V-band (Fig. 8), SN 1994D displays a slightly narrower peak than do SNe 1989B and 1980N. This is largely due to the fact that we use the time of B-band maximum to match up the three light curves. The V-band peak occurred 2.4 and 2.7 days after the B-band peak for SNe 1989B and 1980N, respectively, but only 0.4 days after the B-band peak for SN 1994D. Using the definition of Δm_{15} given above, we measure $\Delta m_{15}(V)=0.76\pm0.04$ mag for SN 1994D, again placing it in the middle of the distribution, equal within the uncertainties to those of SNe 1989B [$\Delta m_{15}(V)=0.71\pm0.07$ mag] and 1980N [$\Delta m_{15}(V)=0.73\pm0.05$ mag] (both values taken from Table 9 of W94). One must be very careful to define one's terms when comparing decline rates; if we choose to use the time of V-band maximum as the fiducial time, we would *not* conclude that SN 1994D has a narrower peak than the other events. In order to compare light curves properly, one must sample them well both before and after maximum. In V-band, the knee in the light curve is more difficult to discern, since the decline immediately after maximum is more gradual and blends gently into the exponential

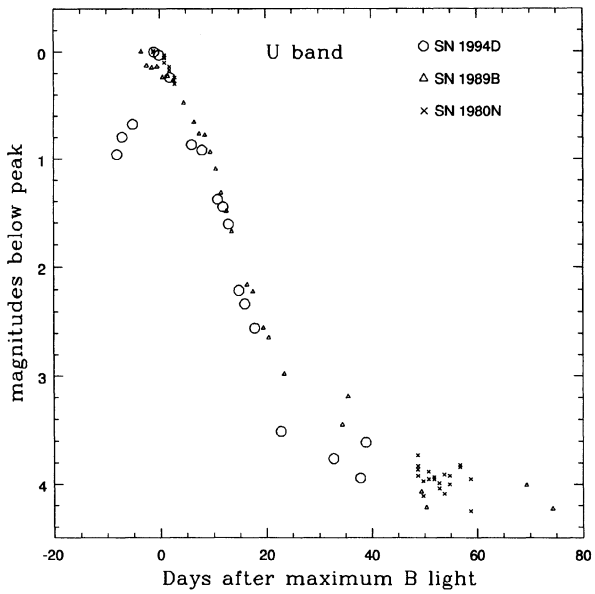

FIG. 6. U-band light curves of SNe 1994D, 1980N, and 1989B.

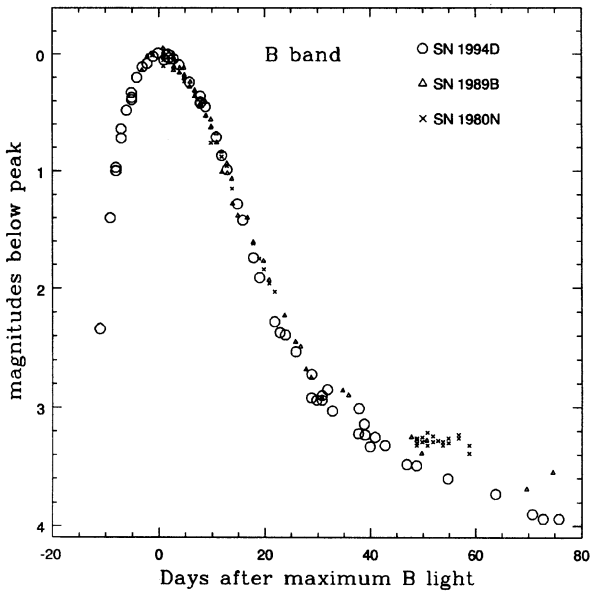

FIG. 7. *B*-band light curves of SNe 1994D, 1980N, and 1989B.

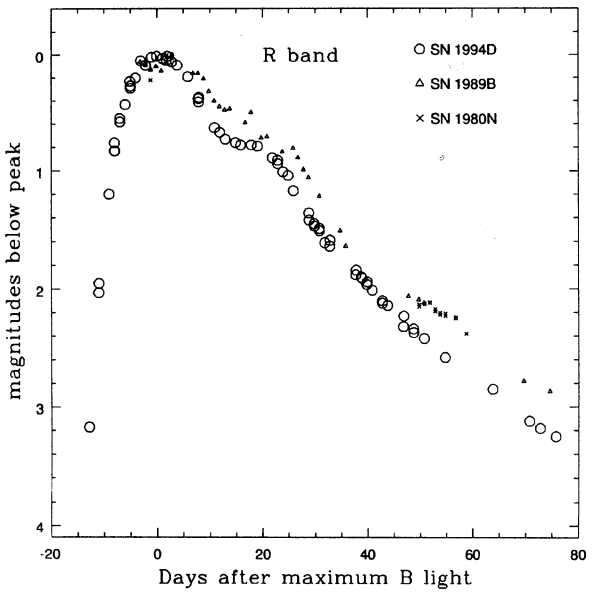

FIG. 9. *R*-band light curves of SNe 1994D, 1980N, and 1989B.

tail. The exponential tail of SN 1994D lies about 0.25 mag farther below the peak than the tails of the other two SNe. There is a subtle decrease in the rate of decline from 14 to 20 days after *B* maximum, which may correspond to the stronger features seen in *R* and *I*.

We show the *R*-band light curve in Fig. 9, in which SN 1994D begins to deviate strongly from a simple decline after maximum. From 14 to 19 days after *B* maximum, the *R*-band light curve remains virtually constant, forming a "shoulder" seen in most other well-observed Ia SNe in the *R*-band (Ford *et al.* 1993; W94). After this pause, the curve dives briefly downwards at about 0.08 mag per day; this drop occurs at the same time as the subtle feature in the *V*-band curve. SN 1994D has a slightly narrower peak in the *R*-band than do SNe 1989B and 1980N. We find $\Delta m_{15}(R)=0.76\pm0.02$ mag. After about 15 days, the shape of SN 1994D's light curve mimics that of the other SNe fairly well, but its exponential tail falls ~0.35 mag farther below the peak.

A secondary peak characterizes the *I*-band light curve (Fig. 10). SN 1994D, like most other well-studied type Ia SNe (SNe 1989B, W94; 1992bc and 1992bo; Maza *et al.* 1994), reaches its first peak in the *I*-band several days before that of the *B*-band curve. Note, however, that SN 1980N seems to reach its first peak *after* the *B*-band peak. We mea-

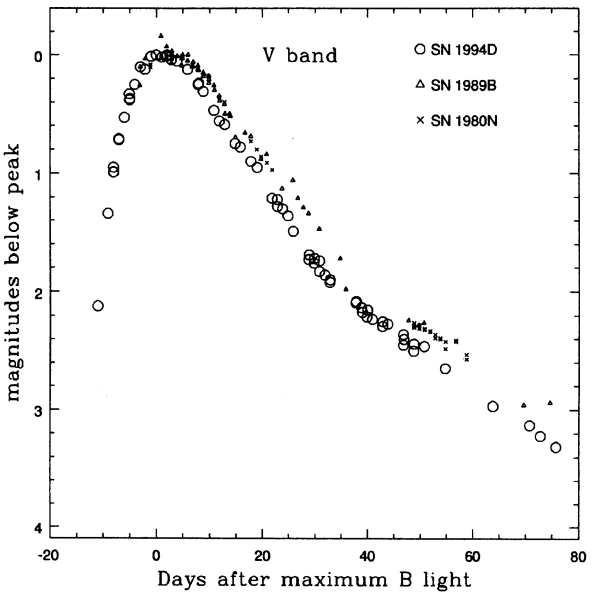

FIG. 8. *V*-band light curves of SNe 1994D, 1980N, and 1989B.

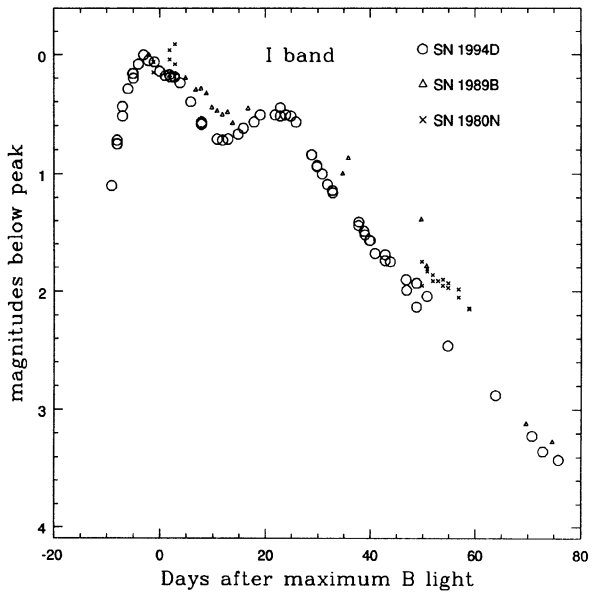

FIG. 10. *I*-band light curves of SNe 1994D, 1980N, and 1989B.

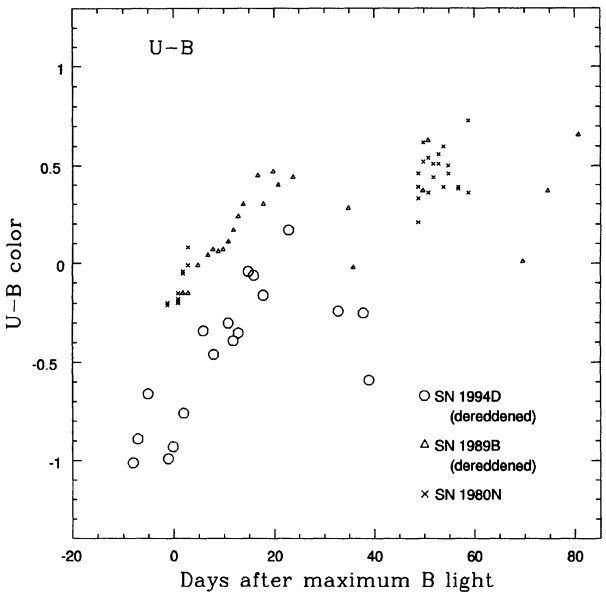

FIG. 11. $(U-B)$ color curves of SNe 1994D, 1980N, and 1989B. The data for SN 1994D have been dereddened by -0.04 mag. The data for SN 1989B have been dereddened by -0.29 mag (W94). The U-band measurements for SN 1994D may be systematically too bright by up to 0.5 mag.

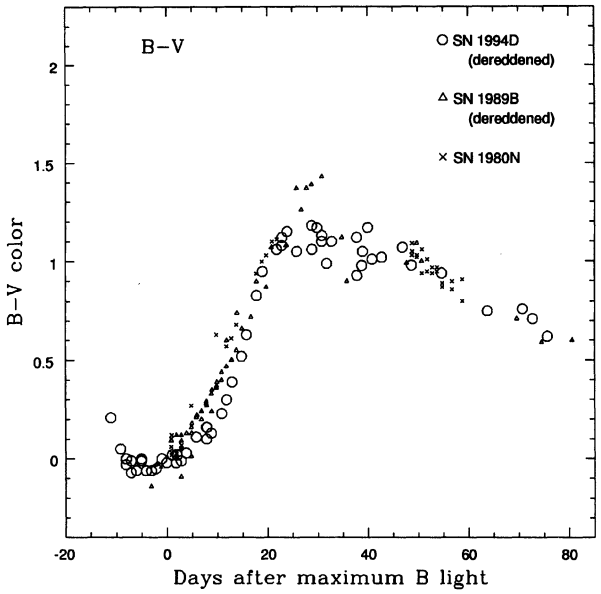

FIG. 12. $(B-V)$ color curves of SNe 1994D, 1980N, and 1989B. The data for SN 1994D have been dereddened by -0.04 mag. The data for SN 1989B have been dereddened by -0.37 mag (W94).

sure $\Delta m_{15}(I)=0.71\pm0.05$ for SN 1994D. The second peak occurs about 23 days after B-band maximum, and is about 0.5 mag fainter than the first. As Maza *et al.* (1994) point out, the location of this secondary maximum is not identical in all type Ia SNe. It may be significant that SNe 1994D and 1992bo with values of $\Delta m_{15}(B)$ of 1.33 and 1.61 mag, respectively, have similar secondary I-band peaks: roughly 20 days after B maximum and 0.4 mag below the first peak. The slowly fading SN 1992bc, with a much smaller $\Delta m_{15}(B)=0.89$ mag, had a later (30–35 days after B maximum) and weaker (0.8 mag below primary I-band peak) secondary maximum. Another slowly fading [$\Delta m_{15}(B)=0.94$ mag] object, SN 1991T, is less atypical: it reached a second peak in I-band about 24 days after B maximum, and only 0.37 mag below the primary I-band peak (Wells 1994). The subluminous and spectrally peculiar type Ia SN 1991bg, which declined *very* quickly [$\Delta m_{15}(B)=1.88$ mag], displayed no secondary maximum at all (Leibundgut *et al.* 1993; Filippenko *et al.* 1992). We agree with Maza *et al.* (1994) that type Ia light curves in the I-band vary substantially, making template-matching impractical.

In summary the light curves of SN 1994D closely resemble those of the normal type Ia SNe 1989B and 1980N. SN 1994D exhibits a slightly narrower peak and quicker decline in V, R, and I, and an exponential tail fainter relative to the peak.

5. OPTICAL COLOR CURVES

We present the color curves, $(U-B)$, $(B-V)$, $(V-R)$, and $(R-I)$, for SN 1994D in Figs. 11–14. Once again, we plot days after maximum light in the B-band on the abscissa; we plot the observed colors on the ordinate. We also show data from the normal type Ia SNe 1989B and 1980N for comparison. We correct the SN 1994D data for a color excess of $E(B-V)=0.04$ mag (which we derive below), and follow W94 in correcting the data for SN 1989B for a reddening of $E(B-V)=0.37$ mag. We make no corrections to the data for SN 1980N. In the discussion below, we denote any dereddened quantity with a zero superscript, such as $(B-V)^0$; values which lack the superscript are not corrected for reddening.

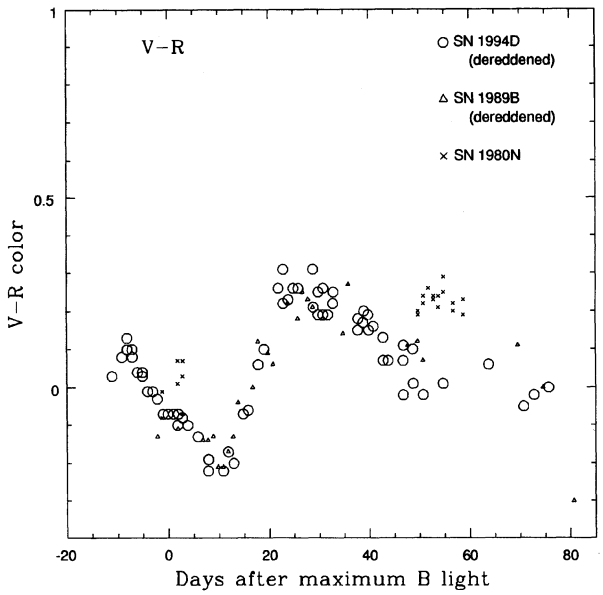

FIG. 13. $(V-R)$ color curves of SNe 1994D, 1980N, and 1989B. The data for SN 1994D have been dereddened by -0.03 mag. The data for SN 1989B have been dereddened by -0.30 mag (W94).

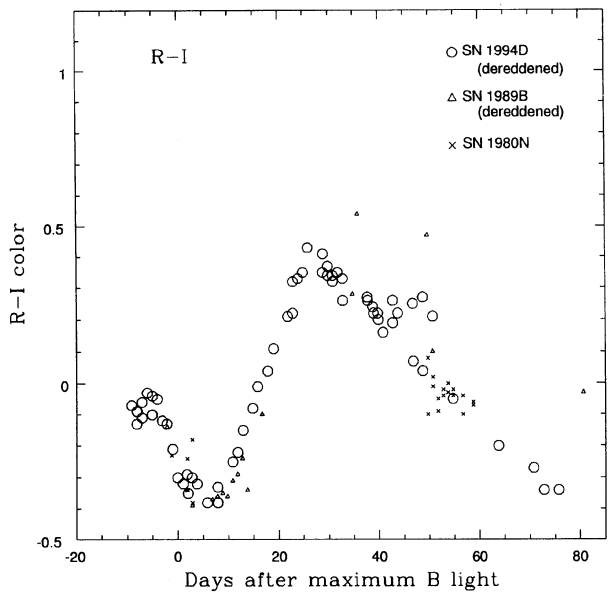

FIG. 14. $(R-I)$ color curves of SNe 1994D, 1980N, and 1989B. The data for SN 1994D have been dereddened by -0.03 mag. The data for SN 1989B have been dereddened by -0.29 mag (W94).

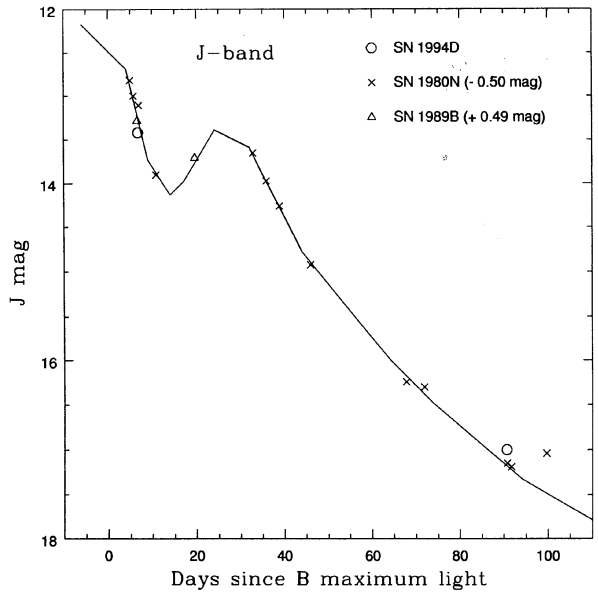

FIG. 15. J-band light curves for SNe 1994D, 1980N, and 1989B. The line shows the template curve for type Ia SNe of Elias *et al.* (1985). The data for SN 1989B have been dereddened following W94.

The $(U-B)$ curve (Fig. 11) shows SN 1994D to be much bluer than either of the other SNe. It is possible that an error in the calibration of the SN 1994D U-band data (gathered exclusively by the Leuschner 50 cm telescope) is responsible for this difference; certainly the U-band measurements are less accurate than those in any other bandpass. The earliest measurement, made about eight days before B maximum, finds SN 1994D at $(U-B)=-0.97$ mag. At the time of B maximum, the color is roughly the same [note that the datum 5 days before B maximum, $(U-B)=-0.62$ mag, was measured through clouds]. After maximum light, SN 1994D remained about 0.4 mag bluer than the other SNe.

Measurements of the $(B-V)$ color are more precise, and Fig. 12 shows a well-defined curve that conforms fairly well to that of the other two SNe. SN 1994D and SN 1980N have very similar colors, while SN 1989b shows slightly more extreme values. At the time of B maximum, SN 1994D had an observed color $(B-V)=-0.01$ mag, corresponding to an intrinsic color $(B-V)^0=-0.05$ mag for $E(B-V)=0.04$ mag. Note that the color was decreasing at the time of discovery, reaching a minimum of $(B-V)^0=-0.07$ mag about five days before maximum light in B.

The $(V-R)$ (Fig. 13) and $(R-I)$ (Fig. 14) color curves follow similar patterns, growing bluer before B-band maximum and a short time thereafter, reddening until the time of the secondary I-band peak, then slowly growing bluer again. In both graphs, the SN 1994D points lie close to those of SNe 1980N and 1989B.

6. NEAR-IR LIGHT CURVES

Since we have only two epochs of data on SN 1994D in the near IR, we are unable to perform a rigorous analysis. Nonetheless, we will compare our observations with the light curves available from the literature, checking for consistency, if nothing more.

We present our infrared observations of SN 1994D in Table 9, and in Figs. 15–17 we plot our observations together with those of SNe 1980N (Elias *et al.* 1981) and SN 1989B (W94). We include the mean light curves of type Ia SNe in the IR compiled by Elias *et al.* (1985), which have been arranged to fit the extensive data for SN 1980N. In

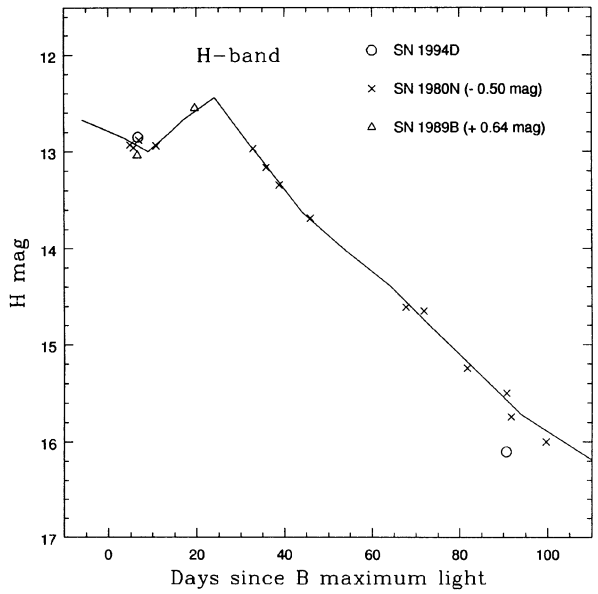

FIG. 16. H-band light curves for SNe 1994D, 1980N, and 1989B. The line shows the template curve for type Ia SNe of Elias *et al.* (1985). The data for SN 1989B have been dereddened following W94.

TABLE 9. IR data on SN 1994D.

Date[a]	J	H	"K"	comments
9438.7	13.42 ± 0.06	12.85 ± 0.06	12.85 ± 0.06	"K" = K (2.2 μm)
9522.6	17.0 ± 0.4	16.1 ± 0.2	15.7 ± 0.15	"K" = K′ (2.1 μm)

[a]Julian Date - 2,440,000.

TABLE 10. Estimates of color excess (mag) to SN 1994D.

method	E(B-V)	calibration	source
log N(Na I) to E(B-V)	$0.044^{+0.027}_{-0.017}$	Sembach et al. 1993	this paper
log N(Na I) to log N(H) to E(B-V)	$0.026^{+0.026}_{-0.013}$	Ferlet et al. 1985 Spitzer 1978	Ho & Filippenko 1995

Figs. 15–17, we plot the observed values for SN 1994D, but shift the other datasets in magnitude (not in days since maximum light). We subtract 0.50 mag from the observed values of SN 1980N in all three bands. For SN 1989B, however, we add amounts which vary with wavelength, since it suffered large amounts of extinction, $E(B-V)=0.37$ mag. We follow W94 exactly in making this correction, using the interstellar extinction curve of Savage & Mathis (1987).

In all near-IR bandpasses, SN 1994D fades by an amount consistent with other type Ia SNe between days 6 and 90 after B-band maximum. The only significant difference is in the H-band, where the datum for SN 1994D at $t\approx 90$ days falls 0.6 mag fainter than expected. However, given the very few observations we have in the IR, and the size of the gap between our two epochs, we conclude that SN 1994D appears to behave roughly like other type Ia SNe.

7. EXTINCTION

We will attempt to derive the amount of interstellar extinction towards SN 1994D in two ways: by comparing its optical colors with those of other SNe, and by measuring the strength of interstellar absorption features in its spectrum. Let us mention at the start that extinction due to material in the Milky Way is likely to be small; Burstein & Heiles (1984) list a value of $A_B=-0.01$ mag for NGC 4526, implying negligible amounts of dust along the line of sight to the SN.

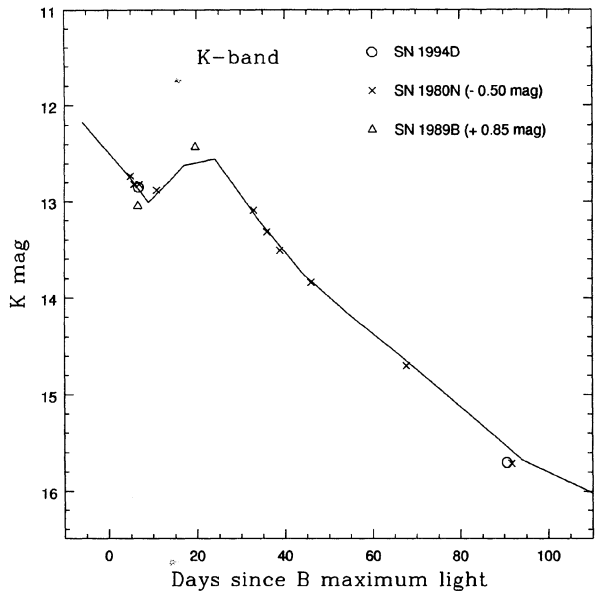

FIG. 17. K-band light curves for SNe 1994D, 1980N, and 1989B. Note that the second datum for SN 1994D was taken at $K'=2.1$ μm. The line shows the template curve for type Ia SNe of Elias *et al.* (1985). The data for SN 1989B have been dereddened following W94.

If we make the assumption that all type Ia SNe have the same intrinsic colors at maximum light, then we can measure the relative amount of extinction between objects very easily. Hamuy *et al.* (1991) suggest that SN 1980N suffered very little extinction, $E(B-V)\leq 0.1$ mag. Comparing the colors at the time of maximum in the B-band, we find a difference of

$$(U-B)_{94D}-(U-B)_{80N}\equiv\Delta(U-B)=-0.70,$$

$$\Delta(B-V)=-0.01,$$

$$\Delta(V-R)=-0.03,$$

$$\Delta(R-I)=-0.04.$$

We are reluctant to use the U-band data for this purpose, since a systematic error is most likely in that bandpass. Discounting $(U-B)$, we find a very small difference between the two SNe. One might reasonably conclude that the difference in reddening is $|\Delta E(B-V)|\leq 0.05$ mag. If SN 1980N truly suffered *zero* reddening (as implied by P93), then SN 1994D must have suffered very little reddening also.

One can also estimate the extinction to a SN by measuring the strength of absorption lines in its spectrum and using a relationship between absorption and reddening derived from stars in our own Galaxy; one must assume that the interstellar medium (ISM) in our galaxy is representative of that in the host galaxy. Ho & Filippenko (1995) acquired high-resolution spectra of SN 1994D and calculated the column density of neutral sodium from the interstellar Na I D absorption features. Taking the total column density they find, one can proceed in two ways to determine the extinction along the line of sight. The simpler method is to apply an empirical relationship between Na I column density and color excess; we use the data of Sembach *et al.* (1993) to find

$$\log E(B-V)=-8.334+0.586\log N(\mathrm{Na}\ I)$$

with a scatter of about 0.18 mag. Alternatively, one can translate Na I into total hydrogen column density, $N(\mathrm{H})=2N(\mathrm{H\ I})+N(\mathrm{H_2})$, and apply a relationship between $N(\mathrm{H})$ and color excess; Ho & Filippenko follow this route, which is appropriate for regions of high column density and extinction (such as the highly reddened SN 1994I, which they also observe). We list the results of both methods in Table 10. The largest uncertainty in each is the assumption that neutral sodium has the average cosmic depletion factor, and so the derived uncertainties are very similar. Noting the asymmetric uncertainties in each measurement, we choose a compromise value of $E(B-V)=0.04\pm 0.03$ mag, with the proviso that the ISM of NGC 4526 is similar to that of the Milky Way. This is consistent with the value derived from

TABLE 11. Adopted extinction (mag) to SN 1994D.

E(B-V)	A_U	A_B	A_V	A_R	A_I
0.04	0.20	0.16	0.12	0.09	0.06

the colors of SNe 1994D and 1980N, and we adopt it for the remainder of this paper. Using the ratios of total extinction to $E(B-V)$ listed in Table 10 of R94, we can calculate the extinction for each bandpass; see Table 11.

8. ABSOLUTE MAGNITUDE

Having measured the peak of each light curve, and found a value for the extinction, we lack only one piece of information needed to calculate the absolute magnitude of SN 1994D: the distance to NGC 4526. This galaxy, located about 6° south of the central clump of elliptical galaxies in the Virgo Cluster, may be a member of the eastern component of the S′ cloud (de Vaucouleurs 1961); Tully–Fisher measurements of several late-type spirals in this component yield a distance modulus of $(m-M)=30.84\pm0.14$ mag (de Vaucouleurs 1994). We prefer to use a more direct method to determine the distance. Observations of surface-brightness fluctuations (SBF) in the bulge of NGC 4526 yield a preliminary distance modulus of $(m-M)=30.68\pm0.13$ mag, placing the galaxy slightly closer than Virgo's central clump of elliptical galaxies (Tonry 1994). We will adopt this distance, 13.7±0.8 Mpc, for all subsequent calculations.

Using the apparent peak magnitudes listed in Table 8, together with our estimate of the extinction and the SBF distance, we calculate the absolute magnitudes of SN 1994D in all passbands and present them in Table 12. The listed uncertainties are a combination of the estimated errors in the observed peak magnitudes, the distance to NGC 4526, and the reddening along the line of sight.

9. IS SN 1994D A "STANDARD CANDLE"?

As Table 12 shows, we find that SN 1994D was more luminous than the normal type Ia SNe 1989B and 1980N, by 0.3–0.4 mag in *BVRI*. In the *U*-band, it exceeded their peak values by ~1.1 mag, but we reiterate that our *U*-band photometry may be systematically too bright by up to half a magnitude. The large difference between SNe 1994D and 1980N is especially significant, as the distance to each was measured by SBF, eliminating any difference in the zero point of the distance scales. The fact that SN 1994D closely resembles normal type Ia SNe in its light curves, yet outshines them, casts some doubt upon the idea that even normal type Ia SNe are standard candles; by this, we mean that it is unlikely that the absolute magnitudes of type Ia SNe comprise a normal distribution with standard deviation $\sigma<0.1$ mag.

TABLE 12. Absolute magnitudes for type Ia SNe.

	U	B	V	R	I	source
1980N	-18.73 ± 0.16	-18.53 ± 0.15	-18.58 ± 0.14	-18.62 ± 0.14	-18.32 ± 0.14	1
1989B	-18.89 ± 0.33	-18.58 ± 0.33	-18.56 ± 0.32	-18.49 ± 0.31	-18.26 ± 0.30	2
1994D	-19.92*±0.36	-18.95 ± 0.18	-18.90 ± 0.16	-18.85 ± 0.15	-18.68 ± 0.14	3

*U-band suffers probable systematic error, up to 0.5 mag too bright.
Sources: 1 – Hamuy et al. 1991; 2 – Wells et al. 1994; 3 – this paper.

P93 has suggested that there is a correlation between rate of decline after maximum and absolute magnitude of type Ia SNe, with slowly fading SNe being more luminous than quickly fading ones. In his Table 2, he calculates linear relationships for the absolute magnitude in *B*, *V*, and *I* as a function of the parameter $\Delta m_{15}(B)$. Applying his formulas to SN 1994D, we find they predict $M_B=-18.19$, $M_V=-18.33$, and $M_I=-18.18$ mag, which are 0.76, 0.57, and 0.50 mag, respectively, fainter than the observed values. Note that, even if there were *zero* extinction to SN 1994D, it would remain more luminous than the predicted values.

Using a set of distant type Ia events with CCD photometry, Hamuy *et al.* (1995) present a similar relationship between absolute magnitude and the $\Delta m_{15}(B)$ parameter. For a sample of type Ia SNe with $0.8<\Delta m_{15}(B)<1.5$ mag, they find slopes in the absolute-magnitude/$\Delta m_{15}(B)$ planes which are smaller than those in P93. They present their results in a form relating *apparent* magnitude, redshift, and $\Delta m_{15}(B)$. This makes it difficult to apply to SN 1994D, whose proximity to the Milky Way and to the Virgo cluster imply that its host galaxy's peculiar velocity is comparable to its motion in the pure Hubble flow. Adopting the SBF distance of 13.7 Mpc to NGC 4526, including the values for extinction we list in Table 11, and following Hamuy *et al.* in using $H_0=85$ km s^{-1} Mpc^{-1} as a fiduciary value, we use their Eqs. (7) and (8) to calculate absolute magnitudes $M_B=-18.35+5\log(H_0/85)$ mag and $M_V=-18.43+5\log(H_0/85)$ mag, which are $0.60+5\log(H_0/85)$ mag and $0.47+5\log(H_0/85)$ mag fainter, respectively, than the observed values for SN 1994D.

Riess *et al.* (1995) describe a method which uses the entire light curve of a SN to determine its absolute magnitude. Unfortunately, their paper does not provide the details necessary to allow readers to use it for themselves, so we cannot comment quantitatively on its application to SN 1994D. As their paper points out, however, it is the portion of the light curve within several weeks of maximum which affects most strongly the derived luminosity. Since the shapes of the light curves of SNe 1994D, 1989B, and 1980N are so similar, all falling clearly into the middle of the "training set" shown in Reiss *et al.*, we conclude that their method of analysis must yield absolute magnitudes for SN 1994D which are very close to those of SNe 1989B and 1980N. Unless the SBF distance to NGC 4526 is substantially too large, the predictions underestimate SN 1994D's actual luminosity.

The alternative to the claim that SN 1994D is superluminous is that the measured distance to NGC 4526 is too large, but we find this explanation somewhat unlikely for two reasons. First, the SBF distance modulus would have to be too large by ~0.6 mag, which would require a large accidental error somewhere in the observations. The method yields uncertainties in individual distance measurements of only 0.16 mag (Jacoby *et al.* 1992); if one were to ascribe the error to an incorrect measurement of the $(V-I)$ color of NGC 4526, it would have to be off by −0.20 mag in order to account for

the error. Second, note that since the difference between predicted and observed magnitudes changes by 0.26 mag from B to I, a single shift in distance barely suffices to bring all three absolute magnitudes within the extremes of P93's predictions. We confess to being wary of the hypothesis that the distance to NGC 4526 *must* be incorrect, for the reason that "otherwise SN 1994D would be more luminous than other SNe Ia;" we believe that observations should be used to support theory, not the converse. In any case, SN 1994D certainly stands as a significant test case. We look forward to further work on the distance to its host galaxy.

Despite the *very* few observations we have in the near IR, we can attempt to compare SN 1994D with SNe 1980N and 1989B in J, H, and K. At these long wavelengths, absorption due to material in the Milky Way and/or the host galaxies is much smaller than in the optical. It is impossible to measure the peak absolute magnitude of SN 1994D in JHK, since we have too few data to identify a peak, much less determine its value. However, we can make a rough guess at the brightness of SN 1994D by *assuming* that its IR light curves are identical to those of other SNe, and then shifting those others to match it. Figures 15–17 show that a reasonable match can be made to SN 1980N if we make it brighter by a constant offset of 0.50 mag; this supports our conclusion that the extinction to SNe 1994D and 1980N are comparable and very small. The difference between the SBF distances to the host galaxies is 0.66 ± 0.18 mag, hinting that SN 1994D was roughly the same brightness as SN 1980N in the near IR. Since there are only two data points for SN 1989B in each bandpass, we note only that, given the distance and extinction to SN 1989B of W94, there is no indication that it differed greatly from SN 1994D in the IR.

Does SN 1994D support the use of type Ia SNe as standard candles? Unless there is a considerable error in the SBF distance to NGC 4526, it is clearly more luminous than the normal type Ia SNe 1989B and 1980N. Moreover, based on its rate of decline, it exceeds the prediction of P93 by ~0.6 mag, and those of Hamuy *et al.* (1995) by ~0.5 mag. The few near-IR observations of SN 1994D hint that it may have a peak infrared luminosity similar to those of other type Ia SNe. We can say with certainty that, *if the SBF distance to NGC 4526 is correct*, SN 1994D does not confirm to the decline-rate/luminosity relationship described in P93 Hamuy *et al.* We feel that the use of type Ia SNe as standard candles is still an open question, one which can be answered only with a much larger sample (~30 objects) of type Ia SNe with both complete light curves and accurate distances.

We thank the referee, Brian Schmidt, for inducing us to work hard and modify our methods of analysis, thereby significantly improving this paper. Brian Taylor and Shawn Baker helped us to acquire images at NURO, and Julianne Dalcanton and Lori Lubin spent valuable Kitt Peak time taking the images we display in our Fig. 1. Andre Martel and Robert Goodrich took the first spectrum of SN 1994D on short notice. We thank Ed Jenkins and Ed Fitzpatrick for their words of wisdom on the ISM. Brian Skiff provided informative messages just days after discovery. Taichi Kato, Bjorn Granslo and their colleagues once again organized observations from around the world into neat collections. M. W. R. thanks the Department of Astrophysical Sciences at Princeton University. L. A. M. and B. D. L. acknowledge the support of the Delaware Space Grant Consortium and Gettysburg College. We are grateful to Sun Microsystems, Inc. (Academic Equipment Grant Program) and to Photometrics, Ltd. for equipment donations that were vital to the acquisition and reduction of data at Leuschner Observatory. Financial support for this research was provided to A. V. F. through NSF Grant Nos. AST-8957063, AST-9115174, and AST-9417213, CalSpace Grant No. CS-96-91, and the Center for Particle Astrophysics (NSF Cooperative Agreement No. AST-8809616).

APPENDIX: LEUSCHNER COLOR TERMS

We followed procedures very similar to those described in the Appendix to R94, including second-order color-dependent extinction corrections *only* for instrumental B-band measurements,[3] we denote the corrected instrumental values by b^0 in the equations below. We have changed the fundamental bandpass from R to V, and removed r from the color term for V, since our R passbands do not match the standard Cousins R very well. We used photometry of the M67 dipper asterism listed in Richmond (1994) to calculate the color terms for both Leuschner telescopes. Note that the bluest star in the M67 asterism has $(U-B)=-0.388$ mag, which is not as blue as SN 1994D in the earliest observations; we are forced to extrapolate the relationship to cover the early SN 1994D data.

We obtained calibration images on the 50 cm telescope in 1993 April, 1994 January, and 1994 October. In the equations below, capital letters denote magnitudes on the standard system, and lower-case letters denote magnitudes on the instrumental system. The terms C_V, C_{BV}, etc., are the differences between the zero points of the instrumental and standard magnitudes, which vary from night to night. Since we always measured the brightness of SN 1994D relative to that of star A, these terms were not involved in the photometric solutions. The color terms are

$$V=v+0.03(b^0-v)+C_V,$$

$$(B-V)=1.15(b^0-v)+C_{BV},$$

$$(U-B)=1.20(u-b^0)+C_{UB},$$

$$(V-R)=0.87(v-r)+C_{VR},$$

$$(R-I)=1.15(r-i)+C_{RI}.$$

We used images of M67 taken in 1994 October and November to calculate the color terms for the 76 cm telescope, finding

[3]Since the SN changes color so drastically [$(B-V)$ changes from ~0.0 mag near maximum brightness to ~1.1 mag 30 days later], this second-order term causes a swing of ~0.06 mag in the B-band magnitude over the course of a month, a significant effect.

$$V = v + 0.01(v-i) + C_V, \qquad (V-R) = 0.88(v-r) + C_{VR},$$

$$(B-V) = 1.16(b^0-v) + C_{BV}, \qquad (R-I) = 1.22(r-i) + C_{RI}.$$

REFERENCES

Argyle, R. W., & Morrison, L. V. 1994, IAU Circ. No. 5976
Burstein, D., & Heiles, C. 1984, ApJS, 54, 33
Casali, M., & Hawarden, T. 1992, JCMT-UKIRT Newslett., 4, 33
de Vaucouleurs, G. 1961, ApJS, 6, 213
de Vaucouleurs, G. 1994, private communication
Elias, J. H., Frogel, J. A., Hackwell, J. A., & Persson, S. E. 1981, ApJ, 251, L13
Elias, J. H., Matthews, K., Neugebauer, G., & Persson, S. E. 1985, ApJ, 296, 379
Ferlet, R., Vidal-Madjar, A., & Gry, C. 1985, ApJ, 298, 838
Filippenko, A. V., *et al.* 1992, AJ, 104, 1543
Filippenko, A. V., Porter, A. C., Sargent, W. L. W., & Schneider, D. P. 1986, AJ, 92, 1341
Ford, C. H., *et al.* 1993, AJ, 106, 1101
Hamuy, M., Phillips, M. M., Maza, J., Suntzeff, N. B., Schommer, R. A., & Avilés, R. 1995, AJ (in press)
Hamuy, M., Phillips, M. M., Maza, J., Wischnjewsky, M., Uomoto, A., Landolt, A. U., & Khatwani, R. 1991, AJ, 102, 208
Hanes, D. A., Harris, W. E., & Madore, B. F. 1976, MNRAS, 177, 653
Ho, L. C., & Filippenko, A. V. 1995, ApJ (in press)
Jacoby, G. H., *et al.* 1992, PASP, 104, 599
Kilkenny, D., & Malcolm, G. 1984, MNRAS, 209, 169
Landolt, A. U. 1992, AJ, 104, 340
Leibundgut, B., *et al.* 1993, AJ, 105, 301
Maza, J., Hamuy, M., Phillips, M. M., Suntzeff, N. B., & Avilés, R. 1994, ApJ, 424, L107
McLean, I. S., *et al.* 1994, in Instrumentation in Astronomy VIII, edited by D. L. Crawford and E. R. Craine (Proc. SPIE 2198), p. 457
Phillips, M. M. 1993, ApJ, 413, L105 (P93)
Prugniel, P., & Heraudeau, P. 1994, private communication
Richmond, M. W. 1994, IAPPP Comm., 55, 21
Richmond, M. W., Treffers, R. R., & Filippenko, A. V. 1993, PASP, 105, 1164
Richmond, M. W., Treffers, R. R., Filippenko, A. V., Paik, Y., Leibundgut, B., Schulman, E., & Cox, C. V. 1994, AJ, 107, 1022 (R94)
Riess, A. G., Press, W. H., & Kirshner, R. P. 1995, ApJ (in press)
Romanishin, W., Ishibashi, K., Morris, A., & Lamkin, M. 1994, IAPPP Comm., 55, 44
Savage, B. D., & Mathis, J. S. 1979, ARA&A, 17, 73
Sembach, K. R., Danks, A. C., & Savage, B. D. 1993, A&AS, 100, 107
Shanks, T., Croom, S. M., & Tanvir, N. R. 1994, IAU Circ. No. 5951
Spitzer, L., Jr. 1978, Physical Processes in the Interstellar Medium (Wiley, New York)
Stetson, P. B. 1987, PASP, 99, 191
Tonry, J. 1994, private communication
Treffers, R. R., Filippenko, A. V., Van Dyk, S. D., & Richmond, M. W. 1994, IAU Circ. No. 5946
Walker, A. 1994, IAU Circ. No. 5950
Wells, L. A. 1994, private communication
Wells, L. A., *et al.* 1994, AJ, 108, 2233 (W94)